Methodology to calculate interfacial tension under electric field using pendent drop profile analysis

Sameer Mhatre,* Sébastien Simon, and Johan Sjöblom

Ugelstad Laboratory, Department of Chemical Engineering, Norwegian University of Science and Technology (NTNU), NO-7491 Trondheim, Norway

E-mail: sameer.mhatre@ntnu.no

Abstract

In this paper we present a methodology to calculate interfacial tension (IFT) of a water-oil interface under electric field. The Young-Laplace equation, conventionally used to estimate surface/interfacial tension in axisymmetric drop shape analysis (ADSA), is modified to include electrostatic effects. The solution needs normal component of the Maxwell stress at the interface which is calculated separately by solving the Laplace equation for electric potential. The optimized fitting between the resulting theoretical profile and the experimentally obtained profile results into Bond number which is used to calculate the apparent value of interfacial tension. The algorithm can process a large number of drop profiles in one go. The methodology can be applied in the ADSA studies for adsorption dynamics where a drop is held for a long time while surface active molecules are allowed to adsorb. The method discussed in this paper will help the future studies in adsorption dynamics at fluid interfaces under electric field and the resulting interfacial property evolution.

Introduction

The knowledge of surface/interfacial tension (γ) is important in the industrial applications involving emulsions and foams. The stability of an interface, which is characterized by the interfacial tension, is crucial for shelf life of pharmaceutical and food emulsions. There exist a large number of techniques to estimate the surface and interfacial tension.[1,2] The drop profile-based methods such as axisymmetric drop shape analysis (ADSA) have been considered superior due to their ability of continuous measurement of interfacial tension (IFT) over a long period of time where the interface is not contacted as in the ring tensiometry. The method involves obtaining the drop profile coordinates and fitting iteratively the Young-Laplace equation to the experimental coordinates by adjusting interfacial tension value.[3] The γ at the best fit between the theoretical profile and the experimental coordinates is considered to be the interfacial tension between the drop phase and the surrounding medium. The drop suspended from a needle tip assumes a shape as a result of equilibrium between gravitational and interfacial forces. Furthermore, the presence of surface active molecules at the interface[4–6] or the influence of additional externally applied forces contribute to the equilibrium drop shape.[7,8] Over the last two decades the literature witnessed a flurry of publications which led to the faster and more accurate techniques.[3,9–11] The erroneous values of the IFT at small Bond numbers is a serious drawback of ADSA. At a lower Bond number the pendent drop becomes more spherical, where a negligible deformation of the drop is equivalent to a large change in the calculated interfacial tension.[12]

The studies on the effect of electric field on surface tension in the absence of surface active compounds have reported contradictory observations. The early investigations suggested that the applied electric field lowers the surface tension of aqueous drops.[13–15] The reported changes in γ under electric fields were substantial. However, a study by Hayes[16] did not find any change in the surface tension in their experiments with water and brine droplets under up to 10 kV/cm. Interestingly, their theory suggested that a strong electric field (> 10 kV/cm) can induce surface tension changes of order 1×10^{-8} N/m which is obviously difficult

to detect in experimental measurements.

The basic assumption in ADSA is that the axisymmetric shape of a pendent drop is determined by an equilibrium between gravity and the surface tension force. The Young-Laplace equation which is balance of these forces across the interface can accurately predict the drop shape. When the drop is subjected to any additional external force, the equation needs modification for it to fit precisely to the real drop profile. The effect of electric field on interfacial properties in multiphase systems has been studied theoretically since long.[17–19] The practical difficulty in experimental investigation of such systems is holding the drop under observation levitated for a long time. The ADSA of a pendent drop under electric field can assist in conducting such experiments; however, the Young-Laplace equation needs to be modified to include the Maxwell stress at the drop interface. Then the calculation of the interfacial properties is similar to the conventional ADSA.

To the best of our knowledge only a few articles reported the methods to estimate IFT by profile analysis of a drop under electric field.[20,21] These studies considered a drop at equilibrium condition where its shape does not change with time. This represents a system void of surface active compound and/or the constant experimental parameters. The theoretical work by Harris and Basaran,[20] to probe stability of a pendent drop under electric field, involved finite element method to solve the Young-Laplace equation and Boundary element method for electrohydrodynamics. Whereas, Bateni *et al.*[21] considered an electrified sessile conducting drop rested on an electrode surface. Panciera *et al.*[22] used a similar method to calculate surface tension during electric field-controlled nanowire growth. The objective of the current manuscript is to present a numerical methodology to calculate dynamic interfacial tension under electric field for a long period of time, where the IFT can evolve for various reasons (our upcoming article will report the IFT evolution in more detail). Novelty of the algorithm lies in its ability to process a large number of drop images in one go. The method will be useful in the accurate measurement of time-dependent interfacial properties of a multiphase system in the presence or absence of an electric field.

The advantage of ADSA over other methods is that a drop can be monitored over a long period of time and its profile can be processed to calculate the interfacial tension as a function of time. We modified the Young-Laplace equation to incorporate electrostatic effects and solved the Laplace equation for electric potential at the drop interface using the experimental boundary conditions. We combined the method with the traditional numerical algorithms to fit experimental drop profiles with the theoretical drop profile by the modified Young-Laplace equation. The algorithm developed in this study processes 3600 drop profiles (drop images captured at 1 frame per second for 1 hour), estimates normal component of the Maxwell stress at the drop interface, generates a theoretical drop profile and estimates apparent interfacial tension by optimally fitting the theoretical profile to the experimental coordinates. As the processing of a large number of drop profiles generated at a set interval is fundamental to the ADSA, the algorithm discussed here has a strong advantage over the previous studies developed for individual images of an electrified sessile drop.[21]

Results and Discussion

A pendent water drop, when surrounded by another liquid, assumes a shape defined by the capillary force and gravity which is a basis for the Young-Laplace equation,

$$\gamma\left(\frac{1}{R_1}+\frac{1}{R_2}\right)=\Delta p_0-\Delta\rho g z, \tag{1}$$

where R_1 and R_2 are principal radii of curvature of the Meridian section of the pendent drop interface as shown in Figure 1. γ and $\Delta\rho$ are the interfacial tension and the density difference of water and medium phases. b is radius of curvature at the drop apex, z and x are vertical and radial coordinates where the origin is assumed to be at the apex. The term Δp_0 represents the pressure difference across the interface at the apex, which is defined as,

$$\Delta p_0=\frac{2\gamma}{b} \tag{2}$$

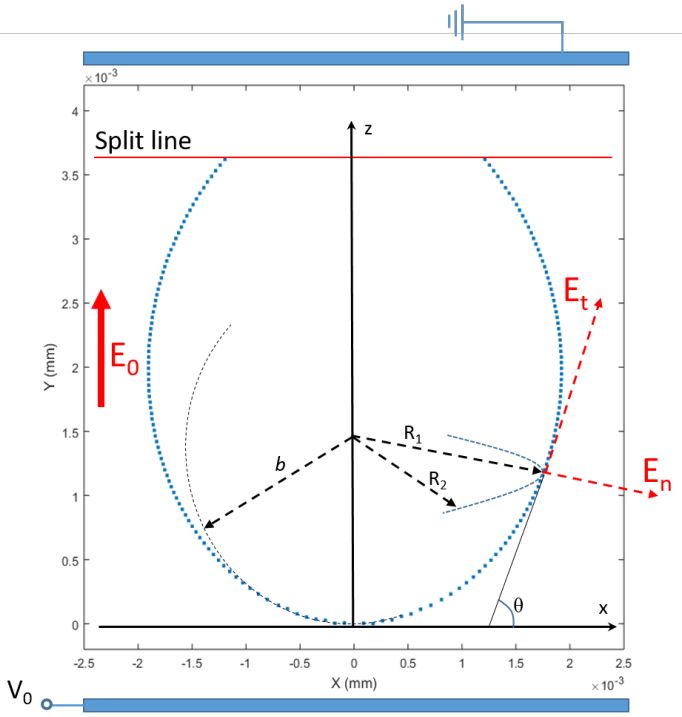

Figure 1: Variables used in the generation of a theoretical profile to fit with the experimentally obtained profile of a pendent drop in electric field.

Modified Young-Laplace equation in electric field

When subjected to an electric field the drop interface experiences additional stresses which must be taken into account in the profile analysis. Equation [1] can be revised as,

$$\gamma\left(\frac{1}{R_1}+\frac{1}{R_2}\right) = \Delta p_0 - \Delta\rho g z + \frac{1}{2}\epsilon.E_n^2. \tag{3}$$

Where the last term on the right hand side of Equation [3] denotes the normal component of the Maxwell stress at the water-oil interface. ϵ is permittivity of the medium phase and E_n is the normal component of electric field E at the drop interface. The tangential component of the electric stresses vanishes in the system where a perfectly conducting drop phase is surrounded by a dielectric liquid.[23] Our algorithm can be applied to the systems where a conducting aqueous drop is held in a dielectric organic liquid.

Given the axisymmetry of the drop shape, the principal radii of curvature in equation [3]

can be written in terms of arc length s as,

$$\frac{1}{R_1} = \frac{d\theta}{ds}, \quad \text{and} \tag{4}$$

$$\frac{1}{R_2} = \frac{\sin\theta}{x}, \tag{5}$$

where θ is the tangential angle as shown in Figure 1. Equation 2 for Δp_o can be revised to the present case as,

$$\Delta p_0 = \frac{2\gamma}{b} - \frac{1}{2}\epsilon.E_n^2\Big|_{s=0}. \tag{6}$$

Combining equations [3], [4], [5] and [6] results,

$$\frac{d\theta}{ds} = \frac{2}{b} - \frac{1}{2\gamma}\left[\epsilon.E_n^2\Big|_{s=0} - \epsilon.E_n^2\Big|_{z(s)}\right] + \frac{\Delta\rho g z}{\gamma} - \frac{\sin\theta}{x}. \tag{7}$$

The tangential component of the Maxwell stress at the drop interface vanishes as the drop phase is conducting. Equation [7] is made non-dimensional by using b as the scaling factor for length and V_0/b for the electric field; the resulting dimensionless equation is,

$$\frac{d\theta}{d\bar{s}} = 2 - \frac{\beta_e}{2}\left[\bar{E}_n^2\Big|_{s=0} - \bar{E}_n^2\Big|_{z(s)}\right] + \beta\bar{z} - \frac{\sin\theta}{\bar{x}} \tag{8}$$

where β and β_e are gravitational Bond number and electrical Bond number, respectively and defined as, $\beta = \frac{b^2\Delta\rho g}{\gamma}$ and $\beta_e = \frac{V_0^2\epsilon_0}{b\gamma}$. β is always negative for a pendant drop and positive for a sessile drop. The non-dimensional variables are denoted by overbars.

Further, the axisymmetric drop profile is characterized by,

$$\frac{d\bar{x}}{d\bar{s}} = \cos\theta, \tag{9}$$

and

$$\frac{d\bar{z}}{d\bar{s}} = \sin\theta. \tag{10}$$

The equations [8], [9] and [10] can be solved for β using initial condition, at apex, $\bar{s} = \bar{x} = \bar{z} = \theta = 0$

Zholob *et al.*[10] argued that the governing equations [8], [9] and [10] can be rewritten into polar coordinates for better accuracy and easier to fit the equations to the experimental drop profile. For the conversion they suggested shifting the origin of the coordinate system to the drop center defined by the point equidistant from the drop apex and the split line. As shown in Figure 2, in the new coordinate system, the center lies on the axis of symmetry at height $z = z_m/2$. Following in the footsteps of Zholob *et al.*,[10] Equation [8] is rewritten in polar coordinate system as,

$$k = 2 - \frac{\beta_e}{2}\left[\bar{E}_n^2\Big|_{s=0} - \bar{E}_n^2\Big|_{z(s)}\right] + \beta\bar{z}_m\Big(1 - \bar{r}\cos\phi\Big) - \frac{1}{\sqrt{1+P^2}}\frac{1}{\bar{z}_m\bar{r}\sin\phi} \tag{11}$$

where,

$$P = \frac{\frac{d\bar{r}}{d\phi}\sin\phi + \bar{r}\cos\phi}{\bar{r}\sin\phi - \frac{d\bar{r}}{d\phi}\cos\phi}. \tag{12}$$

k, in Equation [11], is the curvature, which is defined as,

$$k = \frac{\bar{r}^2 + 2\left(\frac{d\bar{r}}{d\phi}\right)^2 - \bar{r}\frac{d^2\bar{r}}{d\phi^2}}{\left(\bar{r}^2 + \left(\frac{d\bar{r}}{d\phi}\right)^2\right)^{3/2}}. \tag{13}$$

The detailed method of conversion can be found in reference.[10]

Electric field at drop interface

The electric field distribution at the drop interface is estimated independently using 2D finite difference method (FDM). The system solved to get E, shown in Figure 3, is similar to that studied by Harris and Basaran.[20] However, they hybridized the finite element method to solve

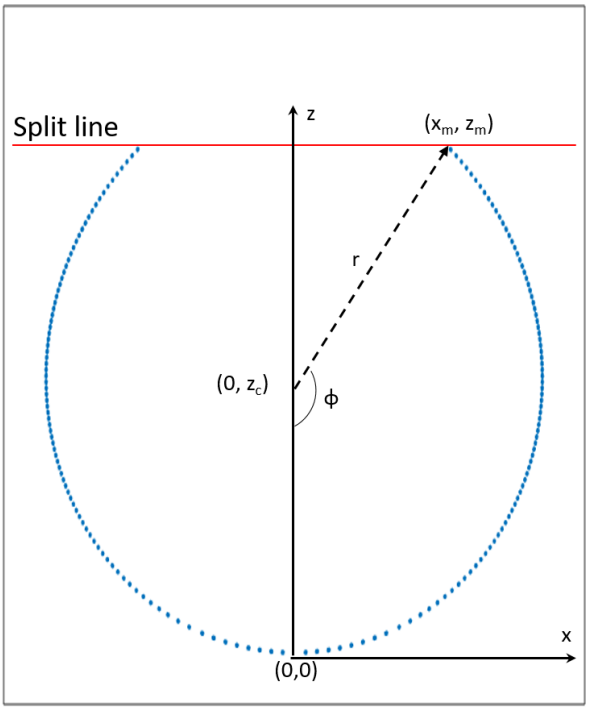

Figure 2: New origin shifted to the drop center in polar coordinates.

the Young-Laplace equation and the boundary element method for electrostatics of a pendent drop. The estimation of the electric field by assuming drop shape to be at equilibrium is straight forward. The solution uses instantaneous experimental drop profile as the drop geometry. The nondimensionalized 2D Laplace equation solved for electric potential outside the drop between two electrode is,

$$\bar{\nabla}^2 \mathrm{v} = \frac{\partial^2 \bar{\mathrm{v}}}{\partial \bar{z}^2} + \frac{1}{\bar{r}} \frac{\partial}{\partial \bar{r}} \left(\bar{r} \frac{\partial \bar{\mathrm{v}}}{\partial \bar{r}} \right) = 0. \tag{14}$$

The lengths in Equation [14] are scaled with diameter of the capillary (c) and electric potential with the applied potential at the lower electrode (v_0). The equation is solved using

following boundary conditions:

$$\bar{\mathrm{v}} = 1 \quad \text{at the lower electrode} A_L \tag{15}$$

$$\bar{\mathrm{v}} = 0 \quad \text{at drop surface D, capillary surface } A_C \text{ and ground electrode } A_G \tag{16}$$

$$n.\nabla\bar{\mathrm{v}} = 0 \quad \text{everywhere in the domain} \tag{17}$$

$$\bar{\mathrm{v}} = 1 - (l+z)/d \quad \text{far-field E, away from the drop} \tag{18}$$

The capillary and drop are randomly kept at zero potential as the capillary is Teflon coated and isolated from the top electrode.

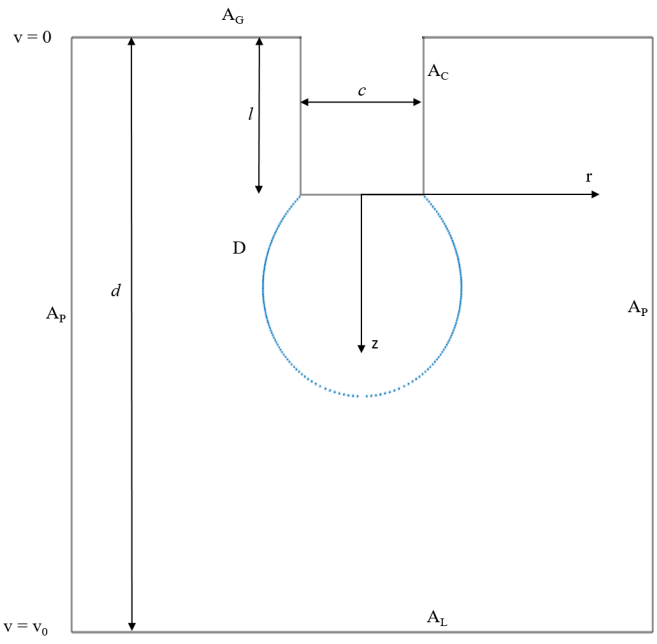

Figure 3: Schematics of the 2D axisymmetric domain used to solve electric field distribution at the drop interface. Boundaries: upper electrode A_G, lower electrode A_L, capillary A_c, periodic boundaries A_p and drop surface D

Algorithm

There exist a number of methods for optimum fitting between two profiles. Rio and Neumann[3] elaborately discussed the various optimization algorithms and criteria of their selection. In the present work we used the Levenberg-Marquardt optimization method to optimize the fit between theoretical and experimental drop profiles. This method is considered advantageous when the initial guess for Bond number is vague. Also, the computation time is fairly small compared to the other optimization methods.

The flow chart of algorithm to calculate apparent interfacial tension when profile coordinates of a drop under electric field is given as an input is shown in Figure 4. A drop of desired size is generated and exposed to a DC electric field. A CCD camera captures images of the drop while the NI tools acquire the images and process them to detect the drop edges and extract the coordinate data at a set rate. The program imports the file containing the coordinate data sets and starts shape analysis from the profile at t=0 s. The experimental drop profile is used to estimate the electric field distribution at water-oil interface separately assuming drop to be rigid. An initial guess for the capillary Bond number (β_0) is needed in the beginning of the solution. In the analysis of subsequent profiles, optimum β of the previous profile is used as the initial guess. The theoretical profile is generated using equation [11] and associated boundary conditions. The Levenberg–Marquardt method optimizes fitting between the theoretical and experimental profiles iteratively by updating β. The optimum β is used to calculate the apparent interfacial tension ($\gamma = \frac{b^2 \Delta \rho g}{\beta}$) and as the initial guess for Bond number for the next profile.

Experiments

The setup used to generate a pendent drop, apply uniform DC electric field, capture the drop images and acquire profile coordinate data is demonstrated by the schematics in Figure 5. The dosing system was used to generate a drop of precise volume and maintain it over

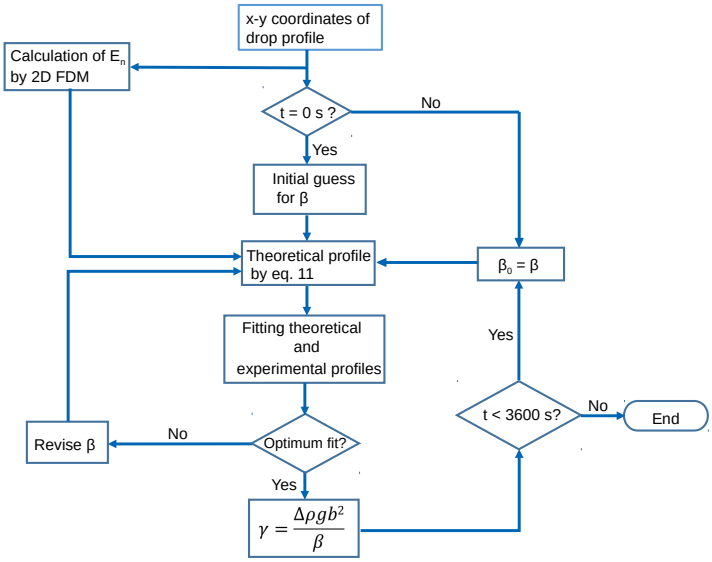

Figure 4: ADSA algorithm to calculate interfacial tension when the pendent drop is under external electric field.

the course of experiment. A Teflon-coated capillary (ID = 1100 μm, OD = 2000 μm and coating thickness = 500 μm) was held vertical between two horizontal steel electrodes such that equator of the drop, created at the opening of the capillary, lies approximately at the centre between the electrodes. The upper electrode was connected to ground and the bottom one to power source. The power source consist of a function generator (Agilent Technologies DSO-X 2022A) and an amplifier (Trek 609E-6).

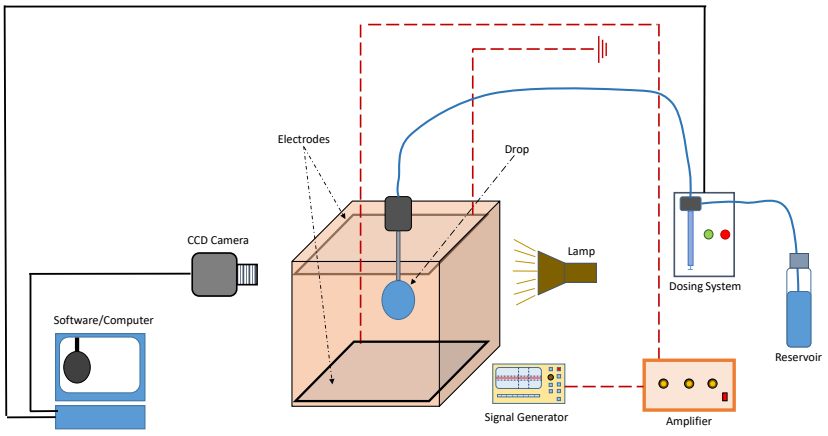

Figure 5: Schematics of the experimental system.

The drop, 3.5 wt% NaCl in Milli-Q water, was surrounded by Xylene (95 %, VWR). The volume of the drop was kept 30 μl in all the experiments so as to avoid errors due to very low capillary Bond number. All the experiments were carried out at room temperature and pressure conditions.

The accuracy of coordinates of the experimental profile is very critical for an accurate calculation of the interfacial tension by ADSA. This paper does not discuss the edge detection technique but a number of studies dedicated to the edge detection can be found in the literature.[24,25] Moreover, several articles on profile tensiometry elaborately discussed the edge detection techniques.[10,26] In our experiments a CCD camera fitted with a Schneider-Kreuznach Componon-S 2.8/50 Enlarging Lens captured the drop image at 1 image per second. The images were acquired by an IMAQ PCI-1408 acquisition board. A gradient-based edge detection scheme IMAQ CannyEdgeDetection[24] was used for image processing and to detect drop edges.

Fitting Experimental Profiles

The CCD camera captured the drop images at 1 frame per second rate for 3600 s. The NI-IMAQ tools acquired the drop images and saved the drop profile coordinate data in a file at the set rate. Each profile, depending on quality of the image, contained between 160 and 200 coordinates. Our interfacial tension calculation code imports the file and fits the theoretical profile calculated by Equation 11 with each time-dependent coordinate data set. At the end of fitting optimization, the apparent interfacial tension is calculated from the corresponding capillary Bond number for each drop profile. Figure 6 demonstrates the experimental and theoretical profiles after the fitting optimization, in the absence (Figure 6(a)) and presence (Figure 6(b)) of the electric field.

The computation speed is governed by accuracy of the initial guess of β. In the system where the interfacial tension does not change significantly over time, the program can be

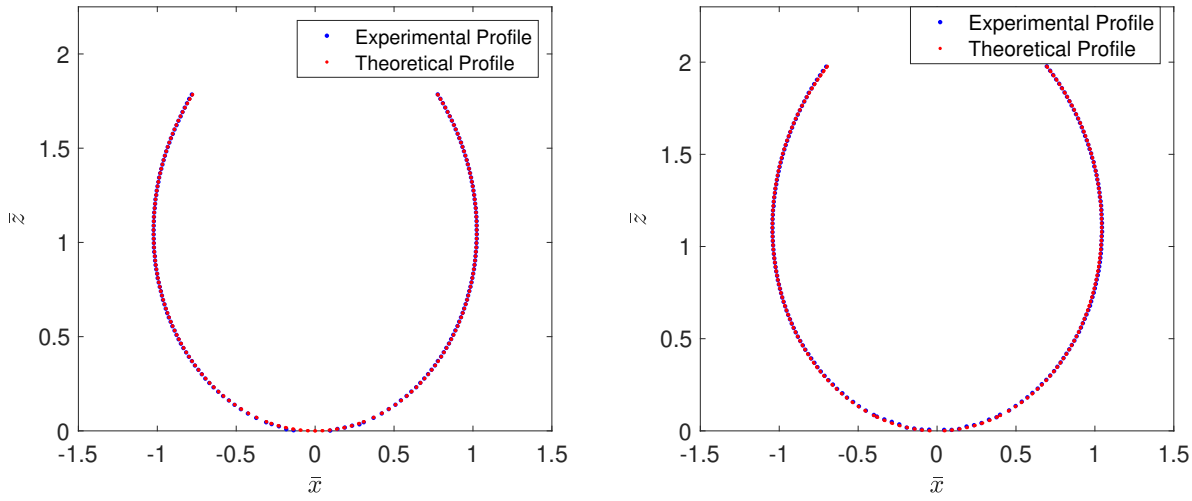

(a) (b)

Figure 6: The modified Young Laplace equation (Equation 11) fitted to the experimental drop profiles. (a) Drop in the absence of electric field, and (b) equilibrium shape of a drop subjected to 0.625 kV/cm.

faster. However, in the studies involving a drop undergoing time-dependent interfacial properties, the program can be made faster by setting optimized β of the previous profile as the initial guess for the next.

In the profile analysis technique when a pendent drop is subjected to an externally applied electric field, the Young-Laplace equation gives inaccurate values of the interfacial tension. As the drop deforms, due to the electric stresses at its interface, the estimated IFT is always less than the real value. As shown in Figure 7, the difference between the real (IFT at 0 kV/cm) and the estimated IFT goes on increasing with strength of the applied electric field. The change can be significant and can give a completely wrong idea of the interface. The accurate values can be obtained by including the Maxwell stress term in the Young-Laplace equation.

The calculated apparent interfacial tension of water-xylene system for an hour is shown in Figure 8. The plots suggest that the γ remains unchanged in both conditions- without electric field and under the field. The initial shape change after the drop subjected to electric

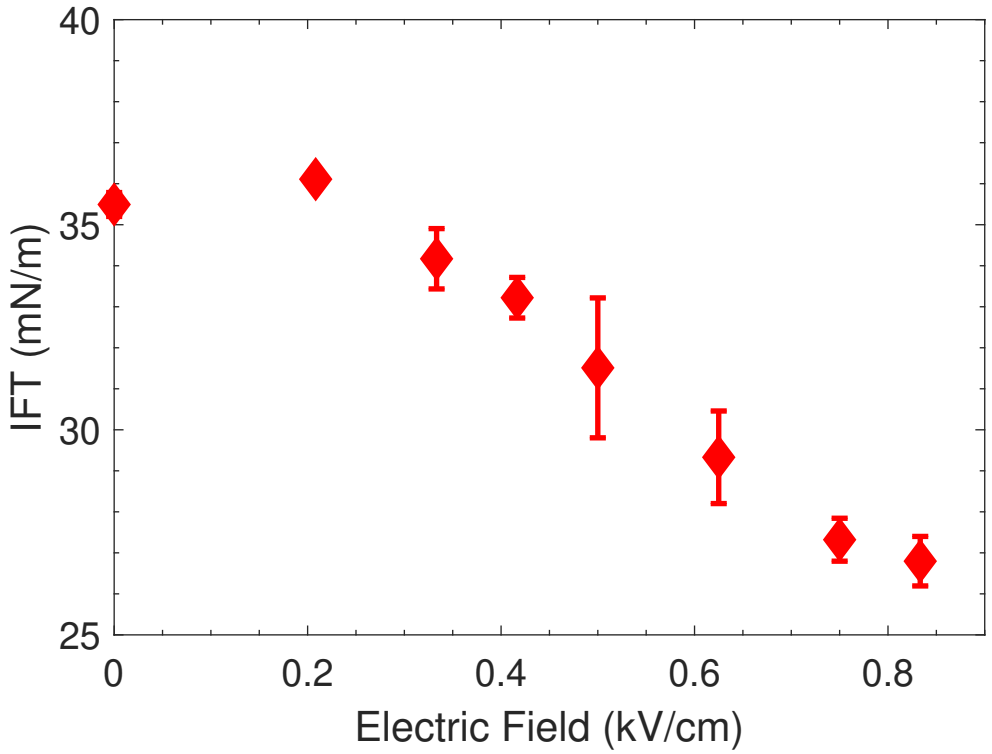

Figure 7: The misleading values interfacial tension of water-xylene interface obtained by the Young-Laplace equation without incorporating the Maxwell stress term.

field is not reflected in the γ plot of Figure 8(b) as it happens within the charge relaxation time ϵ/σ, which is less that 1 s for xylene. Here σ is electrical conductivity of the surrounding phase. The interfacial tension is found to be constant over the range of applied electric field (0-0.833 kV/cm) which is logical given the fact that the fluid system is void of surface active compounds.

Figure 9 shows the apparent interfacial tension which is calculated by taking average of γ from 3600 profiles. The experiment at each electric field is repeated at least 4 times. Additionally, scaling the average values of the apparent interfacial tension under electric field by γ at no field (demonstrated in Figure 10) suggests that the interfacial tension remains constant over a large range of applied electric field.

In addition to the interfacial tension, the numerical fitting calculates geometrical aspects of a drop under electric field. The critical radius of curvature (b), defined as radius of

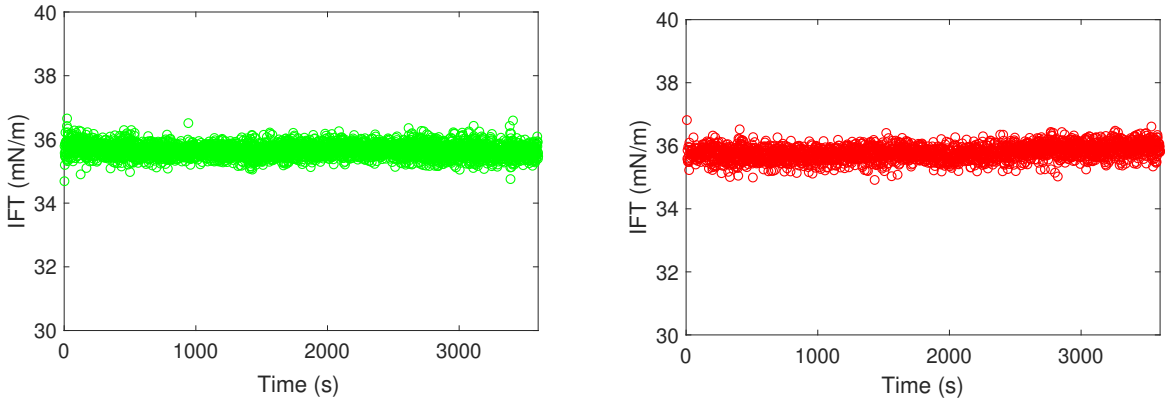

Figure 8: (a) The apparent interfacial tension of water-xylene interface for 3600 s. (b) The apparent interfacial tension of a drop subjected to $E_0 = 0.33$ kV/cm for 3600 s.

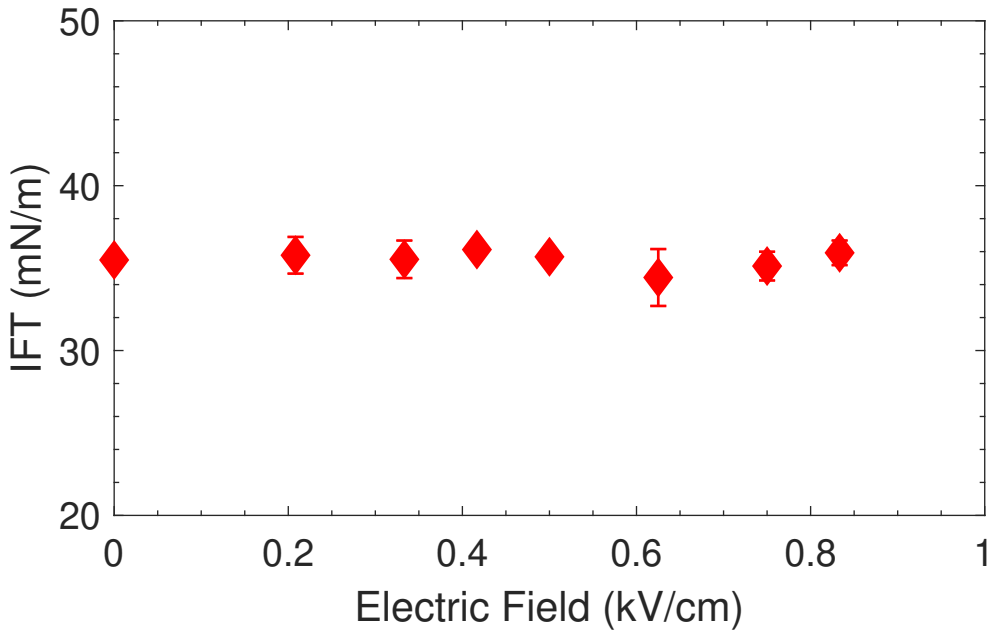

Figure 9: The average apparent interfacial tension of a pendent water drop under electric field for an hour. The error bars are obtained from more than four parallel experimental runs.

curvature of the drop at its apex where the principal radii of curvature (R_1 and R_2) are equal, is other unknown of capillary Bond number. The values of b obtained from fitting of drop profiles under various electric field strengths are plotted in Figure 11. The critical radius

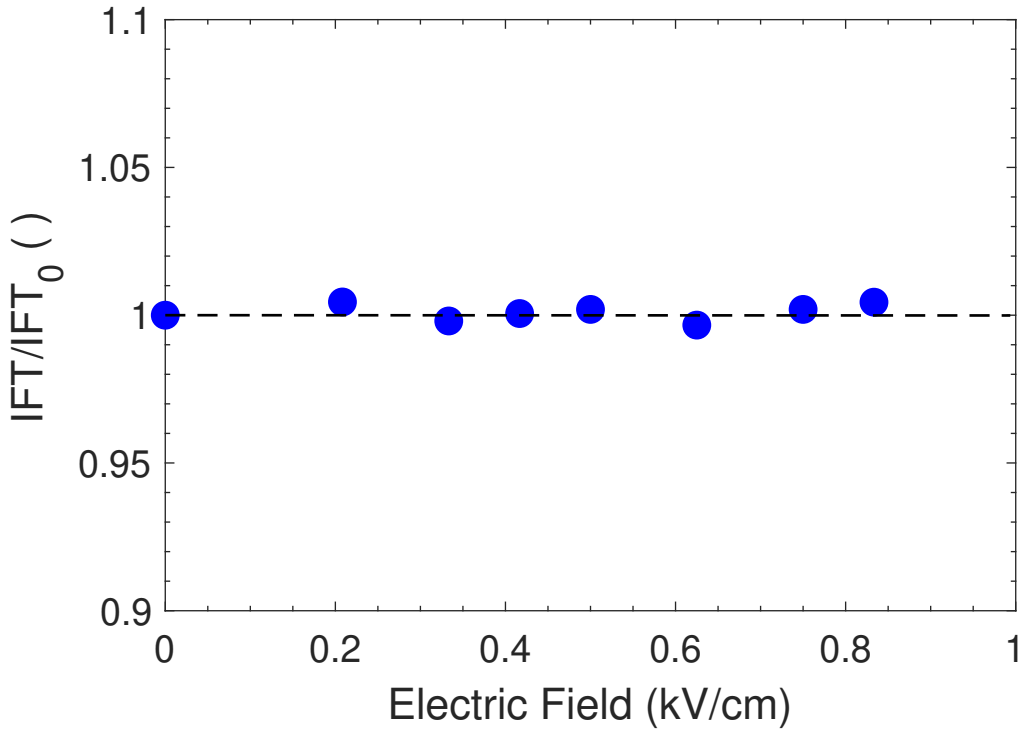

Figure 10: The average apparent interfacial tension under electric field scaled by γ at no field.

appears to monotonically decrease as the applied field is increased. The electric stresses at the drop interface stretch the drop in the vertical direction. The surface charge migration towards the apex, which is already a high curvature part of a pendent drop,[20] ramps up the charge density. The resulting non-uniformity in the charge distribution further increases the radius of curvature at the drop apex. Increasing the magnitude of electric field causes more deformation resulting in to a more tapered apex.

The ADSA is a profile based tensiometry. It assumes that any change in curvature of the drop is due to the change in its interfacial properties. In the absence of electric field, the original Young-Laplace equation (Equation 1) applied to a drop at equilibrium renders a correct estimate of γ. The equation is still valid when the shape evolves over time e.g. by adsorption of surface active molecules to the interface. The continuously evolving drop geometry is captured by a camera and the profiles processed by the conventional algorithms give accurate estimation of IFT. However, when a drop is exposed to an electric field, the

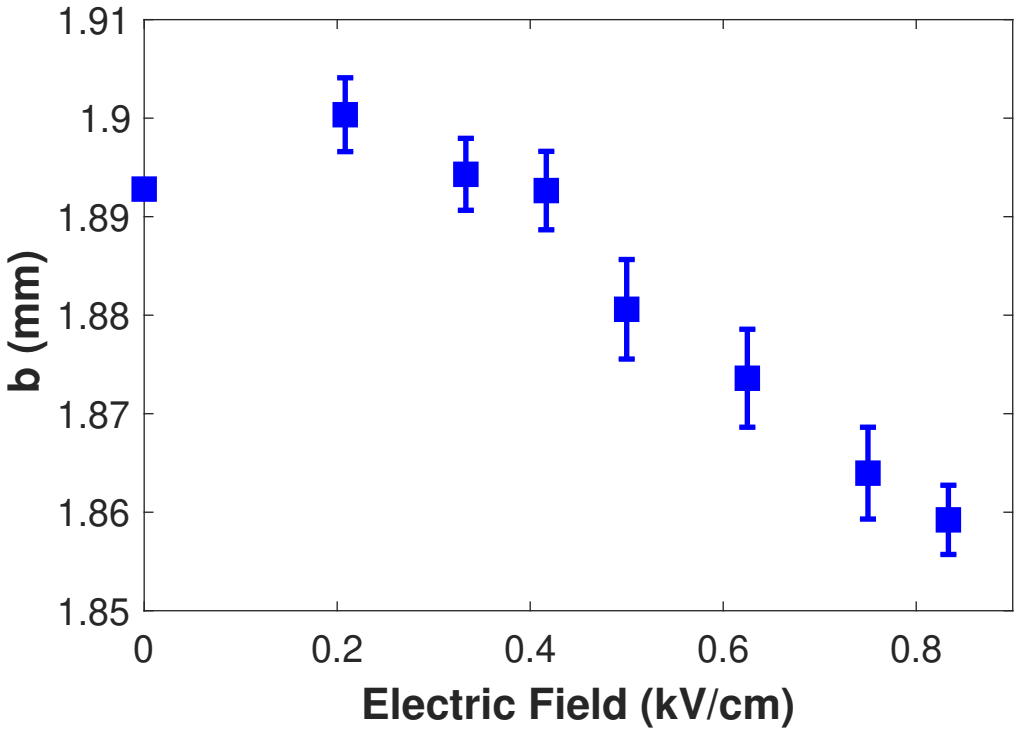

Figure 11: The radius of curvature at apex when the drop is under electric field. The error bars are obtained from more than four parallel experimental runs.

Maxwell stress at its interface are balanced by interfacial tension force and the drop attains a new shape. Although the drop remains at equilibrium thereafter and the new shape is constant, the γ calculated by Equation 1 is less than the real interfacial tension. If not corrected for the Maxwell stress, the Young-Laplace equation accounts the modified geometry for the changing IFT and gives misleading values. Figure 11 shows such electric field dependent curvature at drop apex (b) and the estimated γ by the uncorrected Young-Laplace equation (Equation 1) is shown in Figure 7.

Conclusions

This paper reports a methodology to import and process a large set of pendant drop profiles to extract interfacial tension values. The Young-Laplace equation is modified to include the normal component of electric stress at the drop interface and converted in to polar coordinate

system so as to easily fit with the experimentally obtained drop profiles. The electric field distribution at the drop interface is obtained independently using 2D FDM. The theoretically obtained profile is fitted to the experimental profile using Bond number as a fitting parameter. The interfacial tension is calculated from the Bond numbers at the optimum fit between the two drop profiles. Unlike the previous studies in the surface/interfacial tension calculation under electric field, the algorithm discussed here can handle a large number of images all at the same time.

The apparent interfacial tension, calculated from experimental profiles of an aqueous drop surrounded by xylene, suggests that the applied electric field does not alter the interfacial tension. However, the radius of curvature at the drop's apex decreases upon increasing strength of the applied electric field, further tapering the already high curvature apex of the drop. Our analysis demonstrates that if the Maxwell stress term is not included in the Young-Laplace equation, the estimated interfacial tension can be misleading and significantly lower than the real IFT.

Ethics statement

Ethics statement does not apply to this paper.

Data accessibility statement

All experimental data is presented in Appendix A.

Competing interest statement

We have no competing interests

Authors' contributions

SM did numerical calculations and data processing. SS designed and performed the experiments. JS conceived the study and advised on its theoretical aspects.

Funding

The work is funded by Norwegian Research Council (Grant255174) and industrial sponsors including Nouryon, Anvendt Teknologi AS, NalcoChampion, Equinor and Sulzer.

Acknowledgement

The authors thank the JIP Electrocoalescence consortium "New Strategy for Separation of Complex Water-in-Crude Oil Emulsions: From Bench to Large Scale Separation (NFR PETROMAKS)", consisting of Ugelstad Laboratory (NTNU, Norway), University of Alberta (Canada), Swiss Federal Institute of Technology in Zurich (Switzerland), Institutt for energiteknikk (Norway) and funded by Norwegian Research Council (Grant255174) and the following industrial sponsors – Nouryon, Anvendt Teknologi AS, NalcoChampion, Equinor, and Sulzer.

S. M. would like to thank Dr. Mikael Hammer for helping in data import and processing in Matlab.

Appendix A: Experimental Data

Table 1: Experimental data for an aqueous pendent drop in xylene under DC uniform electric field. η is standard deviation.

Electric Field (kV/cm)	b (μm)		IFT by Young-Laplace equation (mN/m)		IFT by modified Young-Laplace equation (mN/m)	
	Mean	η	Mean	η	Mean	η
0.000	1892.80	0.000	35.493	0.291	35.493	0.291
0.208	1900.35	3.748	36.110	0.042	35.780	1.113
0.333	1894.30	3.652	34.170	0.735	35.533	1.139
0.417	1892.65	3.981	33.220	0.495	36.123	0.299
0.500	1880.60	5.052	31.510	1.706	35.687	0.300
0.625	1873.60	4.973	29.330	1.128	34.430	1.725
0.750	1863.97	4.661	27.320	0.523	35.123	0.874
0.833	1859.23	3.513	26.797	0.603	35.927	0.746

References

(1) Than, P.; Preziosi, L.; Joseph, D. D.; Arney, M. Measurement of interfacial tension between immiscible liquids with the spinning road tensiometer. *Journal of Colloid and Interface Science* **1988**, *124*, 552 – 559.

(2) Drelich, J.; Fang, C.; White, C. In *Encyclopedia of Surface and Colloid Science*; Hubbard, A., Ed.; Marcel Dekker: New York, 2002; pp 3152–3166.

(3) del Rio, O. I.; Neumann, A. W. Axisymmetric Drop Shape Analysis: Computational Methods for the Measurement of Interfacial Properties from the Shape and Dimensions of Pendant and Sessile Drops. *Journal of Colloid and Interface Science* **1997**, *96*, 136 – 147.

(4) Stone, H. A.; Leal, L. G. The effects of surfactants on drop deformation and breakup. *Journal of Fluid Mechanics* **1990**, *220*, 161–186.

(5) Li, X.; Pozrikidis, C. The effect of surfactants on drop deformation and on the rheology of dilute emulsions in Stokes flow. *Journal of Fluid Mechanics* **1997**, *341*, 165–194.

(6) Ha, J.-W.; Yang, S.-M. Effect of nonionic surfactant on the deformation and breakup of a drop in an electric field. *JCIS* **1998**, *206*, 195–204.

(7) Allan, R. S.; Mason, S. G. Particle behaviour in shear and electric fields I. Deformation and burst of fluid drops. *Proceedings of the Royal Society of London A: Mathematical, Physical and Engineering Sciences* **1962**, *267*, 45–61.

(8) Mandal, S.; Chakraborty, S. Effect of uniform electric field on the drop deformation in simple shear flow and emulsion shear rheology. *Physics of Fluids* **2017**, *29*, 072109.

(9) Hoorfar, M.; Neumann, A. W. Recent progress in Axisymmetric Drop Shape Analysis (ADSA). *Advances in Colloid and Interface Science* **2006**, *121*, 25 – 49.

(10) Zholob, S. A.; Makievski, A. V.; Miller, R.; Fainerman, V. B. Optimisation of calculation methods for determination of surface tensions by drop profile analysis tensiometry. *Advances in Colloid and Interface Science* **2007**, *134–135*, 322 – 329.

(11) Nagel, M.; Tervoort, T. A.; Vermant, J. From drop-shape analysis to stress-fitting elastometry. *Advances in Colloid and Interface Science* **2017**, *247*, 33 – 51.

(12) Berry, J. D.; Neeson, M. J.; Dagastine, R. R.; Chan, D. Y. C.; Tabor, R. F. Measurement of surface and interfacial tension using pendant drop tensiometry. *Journal of Colloid and Interface Science* **2015**, *454*, 226 – 237.

(13) Schmid, G. M.; Hurd, R. M.; S., S. J. E. Effects of Electrostatic Fields on the Surface Tension of Salt Solutions. *J. Electrochem. Soc.* **1962**, *109*, 852–858.

(14) Hurd, R. M.; Schmid, G. M.; Snavely, E. S. Electrostatic Fields: Their Effect on the Surface Tension of Aqueous Salt Solutions. *Science* **1962**, *135*, 791–792.

(15) Blank, M.; Feig, S. Electric Fields across Water-Nitrobenzene Interfaces. *Science* **1963**, *141*, 1173–1174.

(16) Hayes, C. F. Water-air interface in the presence of an applied electric field. *The Journal of Physical Chemistry* **1975**, *79*, 1689–1693.

(17) Oliver, D.; De Witt, K. High Peclet number heat transfer from a droplet suspended in an electric field: interior problem. *International Journal of Heat and Mass Transfer* **1993**, *36*, 3153–3155.

(18) Abdelaal, M. R.; Jog, M. A. Steady and time-periodic electric field-driven enhancement of heat or mass transfer to a drop: Internal problem. *International Journal of Heat and Mass Transfer* **2012**, *55*, 251 – 259.

(19) Abdelaal, M.; Jog, M. Heat/mass transfer from a drop translating in steady and time-periodic electric fields: External problem. *International Journal of Heat and Mass Transfer* **2012**, *55*, 2315 – 2327.

(20) Harris, M. T.; Basaran, O. A. Capillary Electrohydrostatics of Conducting Drops Hanging from a Nozzle in an Electric Field. *Journal of Colloid and Interface Science* **1993**, *161*, 389 – 413.

(21) Bateni, A.; Susnar, S. S.; Amirfazli, A.; Neumann, A. W. Development of a New Methodology To Study Drop Shape and Surface Tension in Electric Fields. *Langmuir* **2004**, *20*, 7589–7597.

(22) Panciera, F.; Norton, M. M.; Alam, S. B.; Hofmann, S.; Molhave, K.; Ross, F. M. Controlling nanowire growth through electric field-induced deformation of the catalyst droplet. *Nat Commun.* **2016**, *7*, 12271.

(23) Taylor, G. Studies in Electrohydrodynamics. I. The Circulation Produced in a Drop by Electrical Field. *Proceedings of the Royal Society of London A* **1966**, *291*, 159–166.

(24) Canny, J. A Computational Approach to Edge Detection. *IEEE Transactions on Pattern Analysis and Machine Intelligence* **1986**, *PAMI-8*, 679–698.

(25) Devernay, F. *A Non-Maxima Suppression Method for Edge Detection with Sub-Pixel Accuracy*; 1995.

(26) Cabezas, M.; Bateni, A.; Montanero, J.; Neumann, A. A new drop-shape methodology for surface tension measurement. *Applied Surface Science* **2004**, *238*, 480 – 484.